Volume 5 JULY, 1934 Number 7

PHYSICS

A Journal of General and Applied Physics

Permeability Changes in Ferromagnetic Materials Heat Treated in Magnetic Fields

G. A. KELSALL, *Bell Telephone Laboratory*

(Received April 12, 1934)

Very high maximum magnetic permeability has been obtained in certain ferromagnetic alloys by slowly cooling them in a magnetic field. In permalloy with 78.5 percent nickel it has thus been raised above 140,000 that is, to the same order as is obtainable by rapid cooling without an applied field. In perminvar with 45 percent nickel, 30 percent iron and 25 percent cobalt this magnetic heat treatment is also found to be effective. It is also shown that the maximum permeability is highest if the testing field is in the same direction as that of the field applied during cooling. In directions at right angles to this, the maximum permeability is decreased. The ratio of the two permeabilities in one instance was over 14 for permalloy, and in another instance nearly 70 for perminvar.

THE experiments here reported were suggested by the result of a test, made about ten years ago, in the course of an extended study on the variation with temperature of the magnetic permeability of permalloy. The usual procedure involved measuring the permeability before and after heating the specimen, which was a toroidal core of rectangular cross section consisting of about 30 turns of 1/8 inch $\times$ 0.006 inch tape. In one run, the permeability of a specimen containing 78.5 percent nickel and the remainder iron (78.5 permalloy hereafter) was measured with a ballistic galvanometer at intervals during the time of heating to and cooling from 600°C and the field used for measurement was left on between readings throughout the entire run. Its intensity, 0.085 oersted, was about that for which the permeability of the previously "double heat treated" specimen[1] was maximum before the test. The permeability finally measured at room temperature was 48,000, whereas the permeability of similar material not subjected to magnetizing forces during the same heating cycle would have dropped to about 15,000. This striking result led us to undertake a long series of tests on 78.5 permalloy and on a perminvar[2] with 45 percent nickel, 30 percent iron and 25 percent cobalt (45–30–25 perminvar hereafter). A few tests were also made on 45, 60 and 70 permalloys, 3.8–78.5 chromium permalloy, 3.8–78.5 molybdenum permalloy, nickel, iron (Armco), 50–50 iron-cobalt and 4 percent silicon steel. The original form of specimen was used in most of this work.

Some of the experiments were done in a magnetic testing furnace[3] which had an annular heating compartment made of lavite. The heating elements were wound non-inductively so that they did not affect the magnetic measurements. The necessary windings for making magnetic tests with a ballistic galvanometer were wound around the outside of the furnace. The magnetizing field was applied during heat treatment by passing a suitable current through one of these windings. In other tests the specimens were placed in an annular lavite box on which the

[1] H. D. Arnold and G. W. Elmen, J. Frank. Inst. **195**, 621 (1923).

[2] G. W. Elmen, J. Frank. Inst. **206**, 317 (1928).

[3] G. A. Kelsall, J. O. S. A. and R. S. I. **19**, 47 (1929).

magnetizing winding was wound, and the heat treatment was carried out in a Hoskins' electric furnace. In both these methods the specimen was subjected to a field having at every point the same direction as the field applied in the magnetic tests.

Tests were also made, in some cases, with the fields during heat treatment at right angles to the fields used in measurement. Here solid rings with circular cross sections were used. A direct current between two points diametrically opposite on the circumference produced, in the major portion of the ring, a circular magnetizing field at right angles to the circumference of the ring, along which, of course, the testing field was applied.

The results on 78.5 permalloy will be given first. It was found that maximum permeabilities of the same order were obtained whether an annealed specimen or a double treated specimen was used. Most experiments were, therefore, made on annealed specimens and only such results are here reported. If an annealed specimen is raised to a temperature above the Curie point, which lies for 78.5 permalloy at about 585°C, and if a magnetizing force is applied while the specimen cools slowly, maximum permeabilities are obtained of the same order as with the regular double treatment. The initial permeability is less than for double treatment. In Table I are given the initial and maximum permeabilities (μ_0 and μ_m) and the magnetizing force at which μ_m is reached for various magnetizing forces used during cooling from 600°. The cooling rate was the same for all these tests and

TABLE I. *78.5 permalloy tape toroid.*

Magnetizing force used during cooling from 600°C	μ_0	μ_m	H for μ_m
0 a.c.*	3150	14,300	0.384
0.10 a.c.	2700	46,500	0.1258
0.20 a.c.	2100	64,100	0.0961
0.40 a.c.	2800	81,750	0.0814
0.80 a.c.	2400	95,300	0.0695
1.47 a.c.	3700	100,500	0.0650
2.96 a.c.	4000	100,600	0.0620
10.35 a.c.	3000	98,500	0.0620
2.96 d.c.	2900	100,500	0.0620
1.00 d.c.	2400	98,200	0.0650
0.20 d.c.	2000	68,900	0.0887

* A frequency of 60 cycles was used for (a.c.) magnetizing forces. r.m.s. values are given.

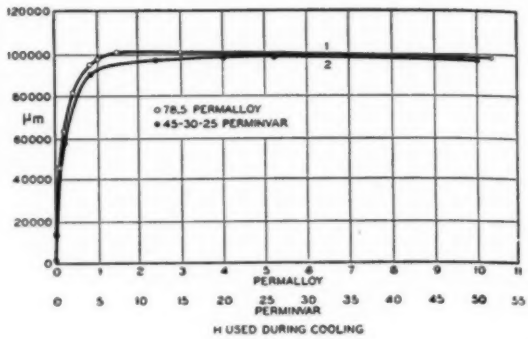

FIG. 1. Maximum permeability of permalloy and perminvar as a function of the magnetizing force applied during cooling.

was such that the specimen cooled from 600° to 200° in about 45 minutes.

Since these treatments left the specimen in a magnetized condition, it was always demagnetized before making the magnetic measurements. The values for maximum permeability are also shown in curve 1 (Fig. 1), plotted against the values of magnetizing force applied during cooling. The maximum increase in maximum permeability is obtained with a magnetizing force of about 1.5 oersteds or more. The data also show that d.c. magnetizing forces are about equivalent to a.c. magnetizing forces of equal r.m.s. values.

In another set of experiments a different but similar specimen was raised to 600°C and an a.c. magnetizing force of 7.4 oersteds was applied at different temperatures, T_a, during successive coolings at the same rate as in the previous experiments. The results are shown in Table II.

Tables III and IV show the result of checking the cooling for one hour and for five hours, respectively, at the temperature chosen for applying the magnetizing force.

TABLE II. *78.5 permalloy tape toroid.*

T_a°C	μ_0	μ_m	H for μ_m
*	4400	20,300	0.235
475	4200	19,980	0.191
500	3460	39,450	0.1397
525	2740	55,600	0.110
550	2550	59,200	0.103
575	2300	60,100	0.103
600	2600	59,300	0.103

*No magnetizing force applied during heat treatment.

Increasing the time of maintaining the temperature at which the magnetizing force is applied increases the maximum permeability obtained and lowers the temperature at which marked increases occur. It is also interesting to note that at or below about 375° substantially the same value of μ_m is obtained whether or not a magnetizing force is applied during the heat treatment. It has been found that if 78.5 permalloy, annealed or double treated, is held at a constant temperature for several days, its permeability (at room temperature) is lowest after baking at about 375°C.

In another set of experiments (Table V) five different specimens of the same lot of material were heated to 600°. A magnetizing force 7.4 oersteds (a.c.) was applied at this temperature and maintained during cooling to room temperature. On arriving at the indicated temperature, T_b, cooling was checked and the temperature maintained constant for five hours.

TABLE III. *78.5 permalloy tape toroid.* Raised to 600°C. On arriving at indicated temperature, 7.4 oersted (a.c.) applied and temperature maintained for one hour. Cooling rate: 600°C to 200°C in 45 minutes exclusive of time held at constant temperature.

T_a°C	μ_0	μ_m	H for μ_m
*	3500	19,310	0.264
400	3600	19,870	0.235
450	3000	81,700	0.0823
475	2480	87,500	0.0808
500	2540	97,200	0.0661
550	2675	104,500	0.0617
575	2540	102,700	0.0617

*No magnetizing force used on cooling.

TABLE IV. *78.5 permalloy tape toroid.* Raised to 600°C. On arriving at indicated temperature, 7.4 oersted (a.c) applied and temperature maintained five hours. Cooling rate: 600° to 200° in one hour and thirty-five minutes exclusive of time held at constant temperature.

T_a°C	μ_0	μ_m	H for μ_m
*		12,520	0.483
373	2200	12,590	0.530
400	3000	22,910	0.308
425	1350	96,700	0.0806
475	1550	94,400	0.0846
510	1650	119,000	0.0684
545	1500	109,100	0.0726

* No magnetizing force used on cooling.

TABLE V. *78.5 permalloy tape toroids.* Raised to 600°C. H applied at 600° and down to room temperature. On arriving at indicated temperature, T_b, temperature was maintained for five hours. Cooling rate: 600° to 200° in 31 minutes exclusive of time held at constant temperature.

T_b°C	μ_0	μ_m	H for μ_m
475	1000	113,500	0.0758
500	1500	126,800	0.0664
525	900	129,000	0.0678
550	1750	140,600	0.0558
565	1700	138,000	0.0568
*	6000	63,500	0.110

* Double treated.

It would thus appear that the highest maximum permeability for 78.5 permalloy is obtained by heating to the non-magnetic temperature or a little above, applying a suitable magnetizing force, cooling to some lower temperature, say 550°, holding the temperature constant for a long period of time, and cooling to about 300°C[4] or lower before removing the magnetizing force.

The effect on maximum permeability of applying transverse fields during heat treatment is opposite to that of applying longitudinal fields. The maximum permeability after applying transverse fields on cooling from 600° is considerably below that which would have been obtained by the heat treatment alone. Tests made using transverse fields are listed in Table VI.

The maximum permeability obtained when using a longitudinal field is over fourteen times that when using a transverse magnetizing field.

In the experiments with 45–30–25 perminvar the temperature was carried up to 725°C (Curie point about 715°C) and the specimens cooled slowly in a d.c. magnetizing field. Tests with a

TABLE VI. *Solid 78.5 permalloy ring of circular cross section. Longitudinal and transverse fields.*

Heat Treatment	μ_0	μ_m
Pot annealed 1100°C	1580	10,500
600°—10 min.—furnace cooled	2300	12,500
600°—10 min.—furnace cooled (a.c.) transverse magnetizing field 15.2*	2000	6,000
600°—10 min.—furnace cooled (d.c.) transverse magnetizing field 15.2*	1900	5,800
600°—10 min.—furnace cooled longitudinal (a.c.) $H=15$	4000	84,000

* Depends on distance from current axis, this is the maximum value in the cross section.

[4] This temperature selected on the basis of other experiments not reported here.

TABLE VII. *45–30–25 perminvar ring.*

(d.c.) magnetizing force used on cooling	μ_0	μ_m
0 longitudinal	383	1,942
0.1 "	300	13,380
1.0 "	165	58,000
4.0 "	170	91,000
12.0 "	500	97,800
20.0 "	790	98,600
26.00 "	890	98,800
50.0 "	900	97,800
8* transverse	660	1,516
†	1570	18,880

* d.c. transverse magnetizing field = 8 (maximum value in the cross section).
† Highest value of μ_m obtained by double treatment.

longitudinal field were made on both tape toroids and solid ring specimens. The results on the two types of cores were of the same general character with the exception that the highest maximum permeabilities for a solid ring were about 25 percent higher than for tape. Table VII shows the results obtained on the solid core for both longitudinal and transverse magnetizing fields.

The values of maximum permeability are shown in curve 2, plotted against magnetizing force used during cooling. The optimum value of magnetizing force during cooling was at least 12 oersteds. The maximum permeability for the longitudinal field is nearly 70 times that for the transverse magnetizing field.

The method of raising μ_m by applying longitudinal magnetizing forces during heat treatment can be applied advantageously to specimens having sizes or shapes inconvenient for producing high permeability by rapid cooling. It is of special interest for the heat treatment of solids of such large cross section that they cannot be cooled rapidly enough and at the same time uniformly enough to avoid severe strains which result in low permeability. One example will serve to illustrate this point. A cylinder of 78.5 permalloy, 12 inches long, 2 inches outside and 1.5 inches inside diameter, intended for a magnetic shield, was double treated. The maximum permeability thus obtained was only 9000. When cooled from 600°C in a magnetic field, the maximum permeability was 111,000.

In the case of nickel, 45 permalloy, 3.8–78.5 chromium permalloy and 3.8–78.5 molybdenum permalloy there was substantially no change attributable to the magnetic treatment. In 60 permalloy there was an appreciable effect and in 70 permalloy μ_m increased from 7290 to 44,300, a change comparable with that in 78.5 permalloy. In 50–50 iron cobalt μ_m increased from 3980 to 6750; in Armco iron from 6950 to 8600; and in silicon steel from 5820 to 8080. Of all the alloys tested, 78.5 permalloy and 45–30–25 perminvar were most affected and these two alloys are also greatly affected by double treatment.

In an article appearing in 1913 Pender and Jones[5] describe experiments made to determine the effect upon its maximum permeability of magnetizing force on silicon steel applied while cooling. The effect they obtained was an increase, greatest when the specimen was heated slightly above the non-magnetic point, and cooled down to about 690° at which temperature an a.c. magnetizing force was applied. An increase in maximum permeability of about 50 percent was obtained in some cases. A similar effect was also obtained with low carbon dynamo steel, but to a lesser degree.

An increase in maximum permeability was similarly obtained in stalloy or silicon steel by E. Wilson.[6] He obtained maximum permeabilities of between 10,000 and 11,000.

Recently R. M. Bozorth and J. F. Dillinger have obtained some remarkable results on 65 and 70 permalloy by performing experiments similar to those here discussed, but in an atmosphere of hydrogen. These are to be described in a forthcoming paper.[7]

In closing I wish to express my appreciation for the valuable assistance of H. J. Williams and R. A. Chegwidden who carried out most of the experiments.

[5] H. Pender and R. L. Jones, Phys. Rev. [2] **1**, 259 (1913).
[6] E. Wilson, Proc. Roy. Soc. **A90**, 343 (1914); **91**, 104 (1914).
[7] Reported at the Meeting of the American Physical Society in Washington, D. C., April 26, 1934.

Space Charge Grid Tube with Variable Mu Grid

WALTER DEHLINGER, *Hygrade Sylvania Corporation, Emporium, Pennsylvania*

(Received April 16, 1934)

Solutions of the generalized equations of the variable Mu triode

$$\exp(pv)=\int_0^{\infty}(v+z)^k F(z)(dx/dz)dz \qquad (a)$$

$$(v+z_0)^n=\int_0^{z_0}(v+z)^k F(z)(dx/dz)dz \qquad (b)$$

for dx/dz are given by means of the gamma-function. Here z is the reciprocal of the amplification constant, x is the axial distance along the grid, v is the ratio of grid to plate voltage and k is the space charge constant, usually 3/2. The constant n or p determines the shape of the plate current, grid voltage curve desired. The only restrictions for the values of n and k are

$$n>k>0 \qquad (c)$$

$$\Pi(n-k-1)\neq\infty. \qquad (d)$$

The solution of the integral equation of the space charge grid tube is reduced to that of the triode by a process of summation. Graphical methods are developed by means of which the distribution of grid pitches can be determined from the solution of the integral equation.

THE distribution of grid pitches necessary for obtaining a desired plate current-control grid voltage characteristic in a space charge grid tube is one of the outstanding problems in designing the variable Mu grid of the electron coupled detector oscillator tubes, the types 1-A-6 and 6-A-7. This problem will be discussed here for the case that the total space current from the cathode does not change over a wide range of control grid voltages. This restriction is very nearly complied with in the pentagrid converters mentioned above as the variation of the total current in these tubes is not more than 30 percent compared with a 10,000 percent change in plate current.

In order to show the principle of designing the variable Mu grid of these tubes more clearly, the following considerations omit the complications arising from the oscillator part of the converter tube and from the fact that the impedance of these tubes is increased by adding a screen grid in front of the plate.

I. ASSUMPTIONS

We assume:

1. Absence of secondary emission.
2. Zero initial velocity of the electrons at the cathode.
3. Zero contact potentials.
4. The distribution of space current between space charge grid and plate is proportional to a power k of the ratio of the voltage applied to the space charge grid and the effective voltage in the control grid.[1]
5. The existence of a simple relation between local grid wire spacing and amplification factor from point to point along the grid.

II. THE RESTRICTED INTEGRAL EQUATIONS FOR THE VARIABLE MU TRIODE

Assume a number of triodes Q of length $\Delta_q x$, which are similar to each other except for their amplification constants $\mu_q=1/z_q$ to be connected in parallel. Let the plate current-grid voltage characteristic of each triode be given by

$$\Delta i_q=P(v+z_q)^k\Delta x_q, \qquad (1)$$

where $v=e_g/e_p$ in the conventional symbols and P is a constant common to all the triodes. The plate current of all the triodes in parallel, $I(v)$, as a function of the modified grid voltage v is thus given as:

$$I(v)=\sum\Delta i_q=P\sum(v+z_q)^k\Delta x_q, \qquad (2)$$

the sum extended over all those triodes for which

[1] This is a generalization of the law for the current distribution between positive electrodes. See: Kusunose, I. R. E. **17**, 1713 (1929). The law is inferred from the consideration, that the lines of force in the tube keep their *distribution* for constant *ratio* of the voltages. Hence the *absolute values* of the voltages for constant voltage *ratio* influences the *intensity only*, the *shape* of the field remains *unchanged*.

for a given value of v the expression $(v+z_q)\geq 0$. The plate current of a triode with an amplification factor decreasing continuously with increasing distance x from the end of the grid axis of total length l is therefore:

$$I(v)=P\int_{z=-v}^{z=l}(v+z)^k dx \tag{3}$$

or, by introducing the variable z:

$$I(v)=P\int_{-v}^{z(\max)}(v+z)^k(dx/dz)dz. \tag{3'}$$

If z is known as a function of the position x along the grid, $I(v)$ can be computed from (3). If, on the other hand, $I(v)$ is given, Eq. (3′) can be solved for dx/dz. By integrating, x can then be found as a function of z, and z as a function of x.

Solutions of Eq. (3′) and the corresponding solutions for z as a function of x have been given[2] for the three following forms of the function $I(v)$: $\exp(pv)$; $(v+z_0)^2$; and $(v+z_0)^{5/2}$. Here z_0 is the value of the negative modified cut-off grid voltage and p is a constant, the logarithmic steepness.

III. Generalization of the Equations for the Variable Mu Triode

We proceed now to the solution of a more general form of variable Mu equation. This generalization concerns two points:

(1) The "kernel" $(v+z)^k$ of the integral equation (3′) is replaced by

$$F(z)\cdot(v+z)^k, \tag{4}$$

where $F(z)$ is an arbitrary function of z which does not contain v; k is only limited by: $k>0$.

(2) The three forms of the desired plate current-control grid voltage characteristic $I(v)$ previously mentioned are replaced by

$$I(v)=A(v+z_0)^n \tag{5}$$ *

for any $n>k>0$ and $\Pi(n-k-1)\neq\infty$. Eq. (5) becomes

$$I(v)=B\cdot\exp(pv) \tag{6}$$

for $A=B(p/n)^n$, $z=n/p$ and $n\to\infty$.

Our problem is the solution of the equations:

$$B\cdot\exp(pv)=P\int_{-v}^{z_0=\infty}(v+z)^k g(z)dz, \tag{7}$$

$$A(v+z_0)^n=P\int_{-v}^{z_0}(v+z)^k g(z)dz, \tag{8}$$

for $g(z)=F(z)dx/dz$. From this it is easy to determine dx/dz and z as a function of x. Some of these solutions are of necessity graphical. The solutions of (7) and (8) are, respectively:

$$g_{ex}(z)=(B\cdot p^{k+1}/P\cdot\Pi(k))\exp(-pz), \tag{9}$$

$$g_n(z)=\frac{A}{P}\frac{\Pi(n)}{\Pi(k)\cdot\Pi(n-k-1)}(z_0-z)^{n-k-1}. \tag{10}$$

These equations follow from the consideration of the gamma-integrals

$$\int_0^\infty \exp(-pt)t^k dt=p^{-(k+1)}\Pi(k) \tag{11}$$

$$\int_0^1 t^k(1-t)^{(n-k-1)}dt=\Pi(k)\Pi(n-k-1)/\Pi(n). \tag{12}$$

By introducing a new variable z into (11) by $z=t-v$, it becomes:

$$\int_{-v}^{\infty}\exp(-p(v+z))\cdot(v+z)^k dz=p^{-(k+1)}\Pi(k).$$

From this (9) follows directly. Similarly by introducing into (12) the variable z by $z=(z_0+v)t-v$, it becomes:

$$\int_{-v}^{z_0}(z_0-z)^{n-k-1}(v+z)^k dz = (v+z_0)^n[\Pi(k)\Pi(n-k-1)/\Pi(n)],$$

from which (10) follows directly.

IV. Mu Distribution in a Space Charge Grid Tube

The current distribution between space charge grid (No. 1) and plate in a space charge grid tube with constant amplification factor is according to our assumption given by:

$$i_p/i_1=a(V_2/e_1)^k. \tag{13}$$

Here a is the ratio of the effective open area to the effective conductive area of the surface of grid No. 1. V_2 is the effective voltage in the surface of the control grid, No. 2, and e_1 is the voltage applied to the space charge grid. The exponent k may be determined experimentally

[2] G. Jobst, Telefunken-Zeitung 17, 29 (1931).

* *Note:* A is a constant.

in a given type of tube. The effective voltage is

$$V_2 = e_2 + e_1 \cdot z_{II} + e_p \cdot z_2. \tag{14}$$

z_2 and z_{II} are the reciprocals of direct and reverse amplification constants of grid No. 2. They can be calculated in a known way from grid pitch and wire size of grid No. 2 and from the geometrical dimensions of grids Nos. 1 and 2 and plate. For constant values of e_1 and e_p the ratio $e_p/e_1 = 1/r$ is a constant. By introducing the symbol z by

$$z = (z_2/r) + z_{II} \tag{15}$$

the effective voltage can be written $V_2 = e_2 + z \cdot e_1$ and the value of V_2/e_1 in (13) becomes:

$$V_2/e_1 = e_2/e_1 + z \cdot e_1/e_1 = v + z. \tag{16}$$

Let the total space current I_{tot} of this tube be independent of the control grid voltage, while space charge grid current $I_1(v)$ and plate current $I_p(v)$ are functions of the modified control grid voltage $v = e_2/e_1$. The total space current of a short length $\Delta_q l$ of the tube of total length l is then equal to $I_{tot} \cdot \Delta_q l/l$. The current distribution between plate and space charge grid of this short length is

$$\Delta_q i_p / [(\Delta_q l/l) I_{tot} - \Delta_q i_p] = a(v + z_q)^k \tag{17}$$

and we find for the ratio of the plate current of the short length $\Delta_q l$ to the total space current of the tube

$$\frac{\Delta_q i_p}{I_{tot}} = \frac{a(v+z_q)^k}{1 + a(v+z_q)^k} \frac{\Delta_q l}{l}. \tag{18}$$

Summing up over all the short lengths $\Delta_q l$ for which the value of $v + z_q \geq 0$, we have

$$\sum \frac{\Delta i_p}{I_{tot}} = \frac{I_p(v)}{I_{tot}} = \sum \frac{a(v+z_q)^k}{1 + a(v+z_q)^k} \Delta x_q, \tag{19}$$

where $\Delta x_q = \Delta_q l/l$. Going to infinitely small $\Delta_q x \to dx$ and replacing the sums by integrals, (19) gives

$$\frac{I_p(v)}{I_{tot}} = \int_{-v}^{z(max)} \frac{a(v+z)^k}{1 + a(v+z)^k} \frac{dx}{dz} dz. \tag{20}$$

We restrict our attention now to an exponential characteristic $I_p(v)/I_{tot} = j \cdot \exp(pv)$, where j is a true fraction; the meaning of j is the ratio $I_p(0)/I_{tot}$. The solution of

$$j \cdot \exp(pv) = \int_{z=-v}^{\infty} \frac{a \cdot (v+z)^k}{1 + a \cdot (v+z)^k} \frac{dx}{dz} dz \tag{21}$$

is

$$dx/dz = j \cdot \exp(-pz) \cdot a^{1/k} / T_k(q) \tag{22}$$

with $q = p/a^{1/k}$. $T_k(q)$ is a function of q and k only. It can be found either by graphical integration of the expression

$$\int_0^{\infty} [u^k/(1+u^k)] \cdot \exp(-qu) du = T_k(q), \tag{23}$$

as indicated in curve No. 1, or by expanding the expression $u^k/(1+u^k)$ into a series, which furnishes

$$T_k(q) = \sum_{n=1}^{N} (-1)^{n+1} q^{n+1} \Pi(nk). \tag{24}$$

The series is asymptotic, the value N is that value of n for which the term $q^{n+1}\Pi(nk)$ has the smallest value. The series development reduces the solution of (21) to the solution of Eq. (7), the generalized exponential triode.

The solution of (21) follows from the consideration of the integral

$$\int_0^{\infty} [u^k/(1+u^k)] \exp(-qu) du = T_k(q),$$

in which the variable z is introduced by the relation $u = a^{1/k}(z+v)$ in a similar way as (9) follows from (11).

Integration of (22) between the limits $x = 0$, $z = 0$ and $x = 1$, $z = \infty$, gives

$$x = (j/q \cdot T_k(q)) \cdot (1 - \exp(-pz)). \tag{25}$$

This gives for $x = 1$, $z = \infty$ the relation

$$j = q \cdot T_k(q) \tag{26}$$

or $j/q \cdot T_k(q) = 1$. The values of j can be read from Fig. 1 (for $k \leqq \frac{1}{2}$). Fig. 2 gives graphically Eq. (25) for $p = 17$, and at the same time the value of z as a function of x. The interesting result is that *it is not necessary to know the value of k for the design of the exponential grid of the space charge tube*, as (25) is independent of the value of $T_k(q)$. The knowledge of the value of k, however, will provide the means to determine the maximum plate current obtainable for a given size tube.

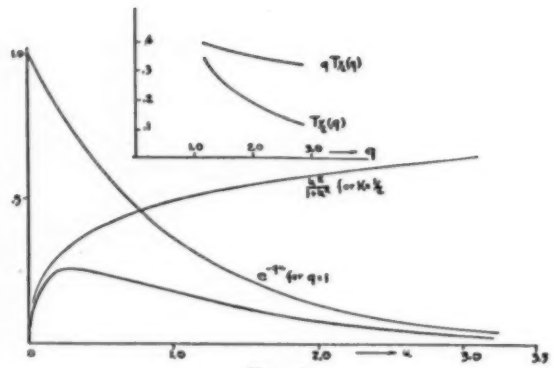

FIG. 1.

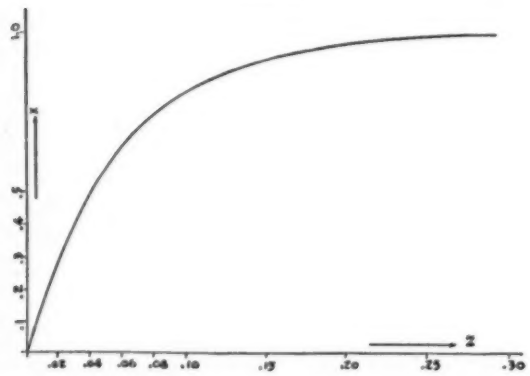

FIG. 2. $x=1-e^{-ps}$ for $p=17$.

V. COMPUTATION OF THE GRID PITCH DISTRIBUTION

In order to wind the grid it is necessary to know the grid wire spacing as a function of the order number N of the turn, counting the turns, e.g., from the turn with the widest spacing in the direction of decreasing spacings. For this purpose we have first to establish a relation between the grid wire spacing y and the variable z of Eq. (25). The formula of Vogdes and Elder[3] serves very well as an illustration. Fig. 3 gives the value of z for a flat construction tube with a control grid made of 0.005″ diameter wire and distances of the control grid of 0.216″ and 0.115″ from space charge grid and plate, respectively. The combination of Figs. 3 and 2 gives the means to construct the curves 4 and 5 of Fig. 4, which represent the relations

$$y=y(x) \qquad (27)$$

and $1/y$ as a function of x. The same curves also represent y and $1/y$ as functions of x'

[3] Vogdes and Elder, Phys. Rev. **24**, 683 (1924).

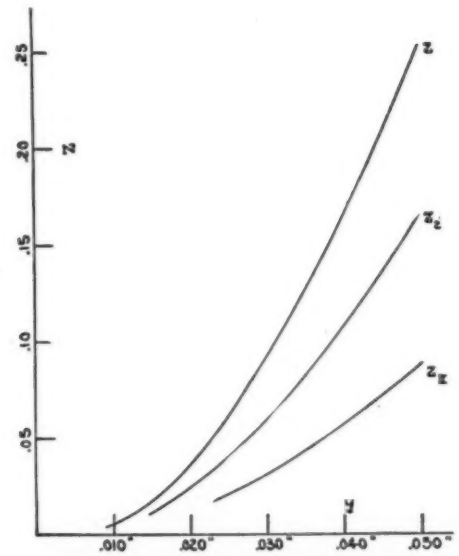

FIG. 3. Value of z for a flat construction tube with a control grid made of 0.005″ diameter wire and distances of the control grid of 0.216″ and 0.115″ from space charge grid and plate, respectively. $z=z_2+z_{II}$. z=reciprocal of amplification factor, calculated as a function of grid wire spacing "y."

$=(1-x)$. A relation between grid wire spacing and order number of the turns is established as follows:

Let n_1 be the number of turns of the largest spacing y_1 and let $y_1>y_2>y_3>\cdots>y_k>\cdots>y_l$. The total number of turns N_k wound up to the end of the last turn of any intermediate spacing y_k is:

$$N_k=\sum_{i=1}^{k} n_i.$$

The length lx' along the grid taken up by these N_k turns is:

$$lx'=l\sum_{1}^{k}\Delta x_i'=\sum_{1}^{k} n_i y_i.$$

Therefore N_k may be expressed in terms of Δx_i and y_i by:

$$N_k=l\sum_{1}^{k}\Delta x_1'/y_1, \quad \text{or} \quad N_k=\int_0^{x'} dx'/y$$

for $l=1$ and continuously variable spacing. Therefore graphical integration of curve No. 5 gives the order number N[4] as a function of x',

[4] The term order number is here used in a generalized sense. It is a *continuously variable* quantity, while "order number" generally means an *integer*.

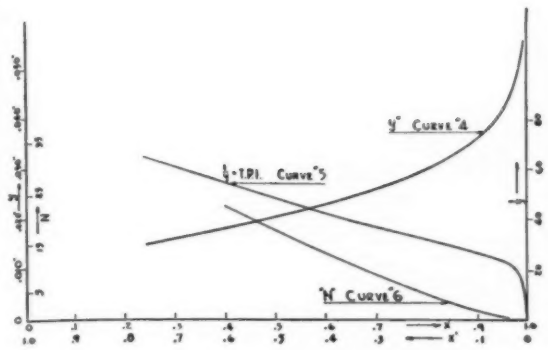

FIG. 4.

see curve No. 6 (Fig. 4). The combination of curves No. 4 and No. 6 gives the means to construct the grid wire spacing y as a function of the order number N, as represented in Fig. 5.

The last step in designing the grid is to replace the continuous curve obtained by the combination of curves No. 4 and No. 6 by a step curve, which assigns a definite pitch to every *integral* order number N.

Different methods can be used for this replacing of the continuous curve by a step curve. Because of considerations on emission, the widest spacing is preferably placed near the middle of the tube axes. This location of the widest spacing leads to the dividing of the tube into two symmetrical sections. The center turn of the grid will be divided into two half turns. Each of these half turns will be the first half turn of the two sections. This is indicated by the Roman figures in Fig. 5. The fact that the wire spacing between two adjacent turns of different pitch varies approximately linear from the middle of one turn to the middle of the next suggests the possibility of approximating the continuous $y-N$ curve in the manner illustrated in Fig. 5 from $N=\mathrm{I}$ to $N=\mathrm{V}$. In the flatter region of the curve where according to this procedure the grid spacings would change by less than say 0.001" from turn to turn, a repeated larger change of spacing will give a smoother approximation to the desired characteristic. This is indicated in Fig. 5 by the step curve for larger values of N.

Obviously the method described here can as well be applied to the design of grids for triodes or pentodes, by a proper choice of the meaning of z. In conclusion, a word may be said about

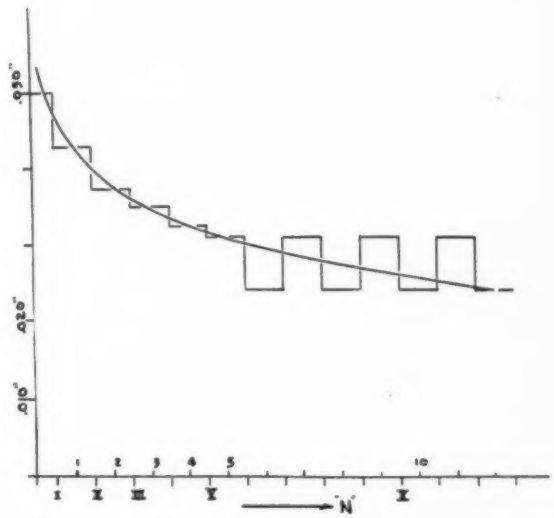

FIG. 5. Find wire spacing "y" (in inches) as a function of the order No. "N" of the turns. Continuous curve, graphical solution; step curve, practical approach to graphical solution.

the meaning of the length l which gives the "scale" for the order number N. This length l is not the actual length of (one section of) the tube. The actual length is shorter because the tube is not operated from cut-off bias all the way down to zero-grid voltage, but only to a specified minimum grid voltage. The flattening of the $y-N$ curve for decreasing values of y indicates that a considerable saving in tube length may result from the specifying of a minimum operating bias. A glance at Fig. 3 gives the minimum grid spacing $z_{\min}$ corresponding to a modified minimum grid bias $v_{\min}=-z_{\min}$. The same curve also gives the maximum grid spacing required for a given cut-off value. The choice of the "scale" l is then fixed by the postulate that one full turn should be obtained for the largest grid spacing. This postulate provides a limitation for the maximum cut-off value which may be combined with a desired logarithmic steepness of the characteristic at a given tube size. Considering the minimum bias and the comparatively small number of variable grid turns in the existing variable Mu tubes we see that a shortening of the length of most of these tubes now in use would not substantially change their characteristics. This shortening will not only permit a saving of space but will also permit a decrease of the filament voltage.

A New Type Long Period Vertical Seismograph

LUCIEN J. B. LACOSTE, JR., *University of Texas, Austin, Texas*

(Received May 7, 1934)

A single spring vertical motion seismograph of theoretically infinite period is described. Actual periods of over a minute have been obtained with a seismograph of this type while for a period of 37 seconds the period was found to be constant to within 1 second for a variation of 9° in the angle between the seismograph arm and the horizontal. A special type of spring is required. The method of winding such a spring is described. A possible method of temperature compensation is given.

I. INTRODUCTION

IT has long been desired to design a long period vertical seismograph in which the period is constant over a considerable range of Ψ, the angle the seismograph arm makes with the horizontal. By using two springs Wilip[1] has eliminated first and second order errors in Ψ while Richardson[2] by a similar method has succeeded in eliminating the third order error also. In the single spring seismograph described in this article all geometrical errors are eliminated for a variation of Ψ of 180°. Fig. 1 is a photograph of the seismograph. It is of the ordinary single spring type but has particular dimensions and requires a special spring. The characteristic of the spring is that its elongation is equal to the distance between the points where it is attached. In other words if the initial length is defined as the actual physical length minus the elongation, then this type of spring has a zero initial length. Springs of this type were easily wound by a method to be described in this article.

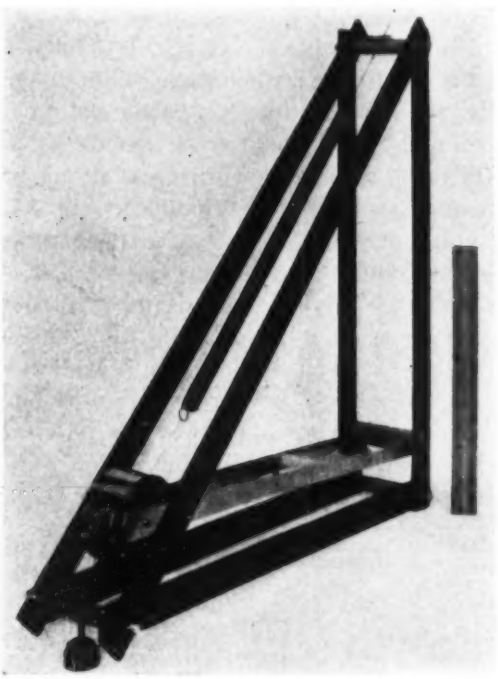

FIG. 1. Photograph of seismograph.

[1] J. Wilip, Gerland's Beiträge zur Geophysik **19**, 387 (1928).
[2] L. F. Richardson, Royal Astronomical Society, M. N., Geophys. Supplement 3, 125, March, 1933.

II. PROOF OF INFINITE PERIOD

A diagram of the seismograph is given in Fig. 2. The weight W is fixed to the arm DC which is pivoted at D. The spring FC is attached to the frame at F and to the arm at C. The lengths FD and DC are taken equal. The point of attachment F of the spring is vertically above the pivot D. The dotted arc FCE is a semicircle with center D.

The proof of the infinite period is as follows. The torque produced by the weight W is $T_w = -Wb \sin \theta$. If it is remembered that the spring is of such a type that its elongation is equal to the distance between its points of attachment, it can be seen that the torque exerted by the spring is $T_s = k(FC)(DG)$, when k = the spring constant. Since $DG = a \sin \alpha$ and

$$FC = FG + GC = a \cos \alpha + a \cos \beta,$$

it follows that $T_s = ka^2 \sin \alpha (\cos \alpha + \cos \beta)$.

Since $FD=DC$, it follows that $\alpha=\beta$ and

$$T_s=2ka^2\sin\alpha\cos\alpha=ka^2\sin 2\alpha.$$

But α is measured by half the arc EC while θ is measured by the whole of this arc; therefore $\alpha=\theta/2$ and $T_s=ka^2\sin\theta$. The total torque on the arm is $T_0=T_s+T_w=(ka^2-Wb)\sin\theta$. If $ka^2=Wb$, then $T_0=0$ for all values of θ, and the period is infinite.

The effect on the period of varying the angle FDH slightly or of adding a small initial length to the spring can be found as follows. Assume that the angle FDH is $90°+\Delta$ and that the initial length of the spring is L; then the total torque becomes

$$T_0=-Wb\sin(\theta-\Delta)+ka^2\sin\theta-Lka\sin(\theta/2). \quad (1)$$

For equilibrium $T_0=0$ and

$$W=\frac{ka^2\sin\theta-Lka\sin(\theta/2)}{b\sin(\theta-\Delta)}. \quad (2)$$

The square of the frequency of vibration is $F^2\alpha-dT_0/d\theta$. From Eq. (1)

$$F^2\alpha Wb\cos(\theta-\Delta)-ka^2\cos\theta+(Lka/2)\cos(\theta/2).$$

Substituting the value of W given in Eq. (2) gives

$$F^2\alpha\frac{ka^2\sin\theta-Lka\sin(\theta/2)}{\tan(\theta-\Delta)}-ka^2\cos\theta+\frac{Lka}{2}\cos(\theta/2).$$

Let $\theta=90°+\delta$. Then, if the arm DC is approximately horizontal, δ is a small angle. By neglecting third order powers of δ and Δ,

$$\sin\theta=1-\delta^2/2,\quad \sin\Delta=\Delta,$$

$$\cos\theta=-\delta,\quad \cos\Delta=1-\Delta^2/2,$$

and $$F^2\alpha\frac{[ka^2-ka^2\delta^2/2-Lka((1+\delta)/2)^{\frac{1}{2}}](\Delta-\delta)}{1-\Delta^2/2-\delta^2/2+\delta\Delta}+ka^2\delta+\frac{Lka}{2}((1-\delta)/2)^{\frac{1}{2}}.$$

By neglecting third order terms in L, δ, and Δ gives

$$F^2\alpha ka^2\Delta+(Lka/2^{\frac{1}{2}})(\tfrac{1}{2}-\Delta+\tfrac{3}{4}\delta). \quad (3)$$

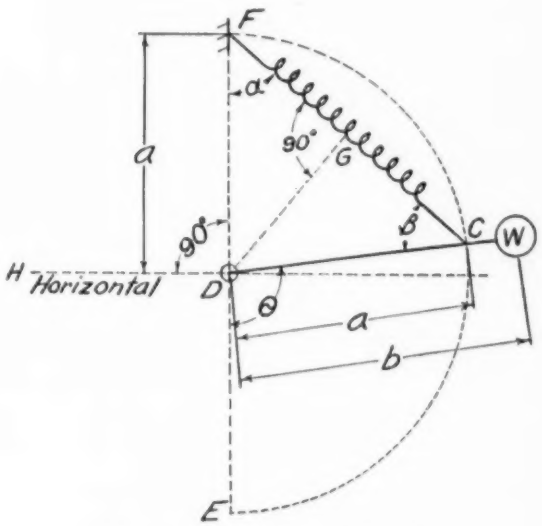

FIG. 2. Diagram of seismograph.

Eq. (3) shows that the period can be shortened either by increasing the angle FDH in Fig. 2 or by giving the spring a positive initial length; this was verified experimentally. It also indicates that the period will depend least on δ, or on θ, if the initial spring length is made zero and the period is adjusted by tilting the seismograph frame. A further conclusion that can be drawn from Eq. (3) is that a monotonic variation of the period with θ can be eliminated by adjusting L, the initial spring length. This has not yet been tested experimentally. A simple method of adjusting L will be described later.

III. Method of Winding a Spring of Negative Initial Length

The method of winding the spring is illustrated in Fig. 3. The bar E is a flat metal bar with a hole drilled through it at ab. The wire used in making the spring passes through this hole and is wound on the mandrel. The bar E is held flat against the spring and at an angle Φ with the direction of the mandrel. As the wire comes out of the hole ab, it must bend at c in order to get in line with the other turns of the spring. This causes the turns to press against each other and give the desired characteristic. The size of the angle Φ and the tension applied to the wire can be found by a few trials. In practice it is not attempted to wind a spring of zero initial length (actual physical length minus elongation). Instead a negative

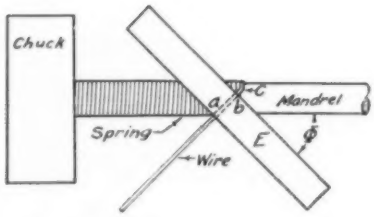

FIG. 3. Method of winding spring.

initial length is obtained and then pieces of wire are added to the spring (as can be seen in Fig. 1) in order to bring the initial length of the combination of spring and wire to zero. If too great a negative initial length is aimed at, it is found that the spring collapses on being stretched. The elongation of a spring can be very easily calculated from the frequency with which a weight attached to it vibrates.

IV. Description of Seismograph Used

In the seismograph shown in Fig. 1 the spring was made of elinvar wire. It was aged for several months by hanging on it the weight that it was to carry in the seismograph. The distances *a* and *b* in Fig. 2 were about 45 cm, and the weight was about 2.5 kg. The pivot consisted of two steel wires, No. 31 B. & S. gauge, clamped on the frame and on the arm. This made an amply rugged pivot. The characteristics of the seismograph were found to depend very little on the size of the wire used for the pivot.

The method of adjusting the seismograph was as follows. A weight was attached to the spring and was set in vertical vibration. The elongation

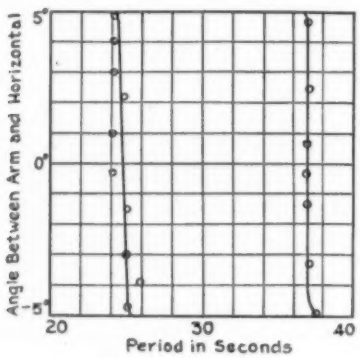

FIG. 4. Variation of period with position of seismograph arm.

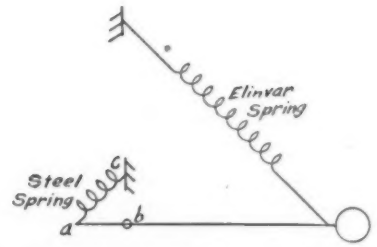

FIG. 5. Possible method of temperature compensation.

of the spring was calculated from the frequency of vibration. Enough wire was then added to the spring to make the length of the combination of wire and spring equal to this elongation. The combination then had zero length. It was placed in the seismograph, and the period was adjusted by tilting the frame.

V. Variation of Period with Position of Arm

Graphs of period against angle of arm are given in Fig. 4. These curves compare very favorably with that given by Wilip.[1] The range of these curves might have been extended had it not been that at the top of the range some of the turns of the spring came into contact with each other, while at the bottom the wire attaching the spring to the arm came into contact with the arm at another point. The data are probably accurate to within one second. Periods of over a minute were obtained with this seismograph, but it was about to become unstable at these periods.

VI. Temperature Correction

When the seismograph was adjusted for long periods, its zero position was found to be very sensitive to temperature changes. Approximate temperature compensation was obtained by adding a small steel spring to the seismograph as shown in Fig. 5. The steel spring was also required to fulfill the requirements of this type of seismograph. The lengths $ab = bc$ were varied until the temperature effects of the two springs approximately balanced each other. This adjustment for temperature compensation has not yet been done accurately, but even with a rough compensation, satisfactory seismograph records have been obtained.

Propagation of Elastic Waves in Ice. Part II

MAURICE EWING AND A. P. CRARY, *Lehigh University*

(Received April 10, 1934)

Flexural waves. A seismograph, used to study propagation of explosion-generated waves in a sheet of ice on a lake, revealed the existence of flexural waves. These waves showed marked dispersion, the group velocity being represented approximately by the empirical formula $U=221(en)^{\frac{1}{2}}$, where e is the thickness of the ice in feet and n is the frequency. A theoretical formula is developed by which the velocity of these waves may be calculated from the elastic constants of ice and water. *Transverse waves.* By a suitable orientation of the seismograph it was possible to detect transverse waves, polarized horizontally, in the sheet of ice. The velocity of transverse waves was found to be 6057 ft./sec. which checks within about three percent with the value of velocity calculated from the elastic constants of ice as reported in Part I.

Apparatus

In connection with measurement of velocity of longitudinal vibrations in ice on a lake it was found that two other types of vibrations could be detected. These are flexural and transverse vibrations. The vibrations were set up by the explosion of a blasting cap placed in a hole in the ice and were recorded by an electric seismograph placed on the ice at suitable distance from the cap. The seismograph used was of the type technically known as a geophone. It was originally designed to measure vertical vibrations only, but minor changes in the spring suspensions have increased its adaptability so that by simply placing it on its side it may also be used to measure horizontal motions.

Flexural Vibrations

Sample records of the flexural vibrations are shown in Fig. 1. These vibrations are interesting because of the beautiful example of dispersion which they offer. They are analogous to surface waves on water, to Rayleigh waves on the surface of a solid or to flexural waves in a bar or thin plate. From inspection of the seismograms it is evident that the group velocity increases with frequency. This relation is shown in Figs. 2–6 where the square root of the period is plotted against travel time for a number of different records. The curves shown in these figures are theoretical curves which will be discussed below.

A preliminary study showed that the relation

$$U=221(en)^{\frac{1}{2}} \tag{1}$$

where U is the group velocity in ft./sec. for waves of frequency n and e is the thickness of the ice in ft., would fit the observed data reasonably well. This may be compared with the known result for the velocity of flexural waves in a thin plate

$$V=2\pi e V_p/12^{\frac{1}{2}}\lambda, \tag{2}$$

where V is the wave velocity for wave-length λ and V_p is the velocity of longitudinal waves in the plate. From the relation

$$U=V-\lambda dV/d\lambda \tag{3}$$

we obtain

$$U=\frac{4\pi e}{12^{\frac{1}{2}}\lambda}V_p=\left(\frac{8\pi V_p}{12^{\frac{1}{2}}}\right)^{\frac{1}{2}}(en)^{\frac{1}{2}}. \tag{4}$$

Taking $V_p=11{,}260$ ft./sec.[1] (4) gives

$$U=286(en)^{\frac{1}{2}}. \tag{5}$$

These Eqs. (2) and (5) give velocities about 20 percent higher than those observed. The effect of the water beneath the ice must be considered.

Choose as the y-axis of a system of rectangular coordinates a line in the equilibrium plane of the ice. Let the x-axis be directed vertically upward. Assume a train of waves in which the vertical displacement of the ice is given by

$$\eta=A\sin(by+ct). \tag{6}$$

[1] *Propagation of Elastic Waves in Ice.* Part I, Physics **5**, 165 (1934).

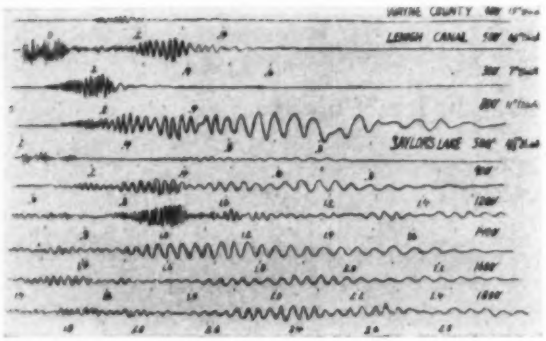

FIG. 1. Sample seismograms of flexural vibrations.

Let Φ, the velocity potential of the water, be given by

$$\Phi = B \cosh d(x+h) \cos (by+ct).$$

It will satisfy the equation of continuity

$$\frac{1}{V_1^2}\left(\frac{\partial^2\Phi}{\partial t^2}\right) = \frac{\partial^2\Phi}{\partial x^2} + \frac{\partial^2\Phi}{\partial y^2} \tag{7}$$

if

$$c^2/V_1^2 = b^2 - d^2,$$

where V_1 is the velocity of longitudinal waves in the water.

The boundary conditions,

$$(\partial\Phi/\partial x)_{x=0} = \partial\eta/\partial t \text{ and } (\partial\Phi/\partial x)_{x=-h} = 0,$$

where h is the depth of the water, are also satisfied provided

$$B = Ac/d \sinh dh.$$

The pressure upon the water can be found from the formula

$$\delta p = -g\rho_1\eta - \rho_1\partial\Phi/\partial t. \tag{8}$$

Assuming the thickness of the ice small compared to the wave-length, the equation of motion of the ice sheet is given by

$$\sigma\partial^2\eta/\partial t^2 = -L\partial^4\eta/\partial x^4 + \delta p \tag{9}$$

where L denotes the flexural rigidity of the ice and σ, the surface density. If e denotes the thickness of the ice and E Young's modulus of elasticity,

$$L = (1/12)e^3[E/(1-\sigma^2)] \quad \text{and} \quad \sigma = e\rho.$$

Substituting these values, together with the pressure given by (8) into (9) and putting $V_p^2 = E/\rho(1-\sigma^2)$ the relation is obtained,

$$V^2 = (F/\lambda^2 + G\lambda^2)/(\rho + (D\lambda/\alpha)\coth(H\alpha/\lambda)), \tag{10}$$

where $F = \frac{1}{3}\pi^2e^2\rho V_p^2$, $G = g\rho_1/4\pi^2e$, $\alpha = (1-V^2/V_1^2)^{\frac{1}{2}}$, $D = \rho_1/2\pi e$ and $H = 2\pi h$ giving the velocity of propagation of waves of length λ in ice of thickness e, resting on water of uniform depth h. This formula may be compared with one obtained by Greenhill[2] for a similar case. Greenhill considered the water incompressible, i.e., $V_1 = \infty$, and used E instead of $E/(1-\sigma^2)$ for determining the flexural rigidity of the ice. To compare Eq. (10) with known results we note that when the thickness of the ice becomes zero and the water is considered incompressible it reduces to the known expression for the wave velocity under the action of gravity. For the density of the water equal to zero it reduces to (2). From (3) and (10) the group velocity of the flexural vibration is found to be

$$U = V\left[1 + \frac{2(F-G\lambda^4)V_1^2\alpha^3\sinh^2(H\alpha/\lambda) + DV^2V_1^2\lambda^3\alpha^2(\sinh(H\alpha/\lambda)\cosh(H\alpha/\lambda) + H\alpha/\lambda)}{2(F+G\lambda^4)V_1^2\alpha^3\sinh^2(H\alpha/\lambda) + DV^4\lambda^3(\sinh(H\alpha/\lambda)\cosh(H\alpha/\lambda) + H\alpha/\lambda)}\right]. \tag{11}$$

This formula has been used to calculate the curves shown in Figs. 2–6. The thickness of the ice varies from 4½ in. to 15 in. and the depth of the water from 4 ft. to 20 ft. in the various curves and the agreement between the observed and calculated values was reasonably good throughout. In making the calculation arbitrary values of wave-length were assumed and by means of successive approximations, the corresponding values of wave velocity were determined from (10). The group velocity was obtained from the wave velocity by (11). The period was obtained from the wave-length and the wave velocity and the travel time was obtained from the distance and the group velocity. Fig. 7 shows the necessity for taking into consideration the effect of the

[2] Greenhill, Am. J. Math. 9, 62 (1887).

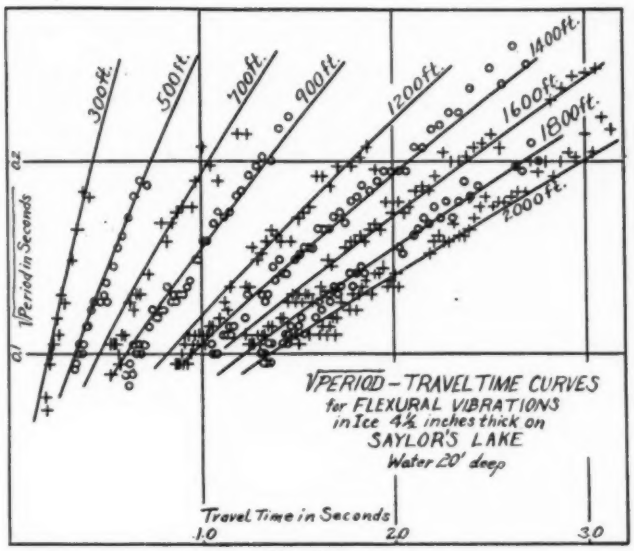

Fig. 2

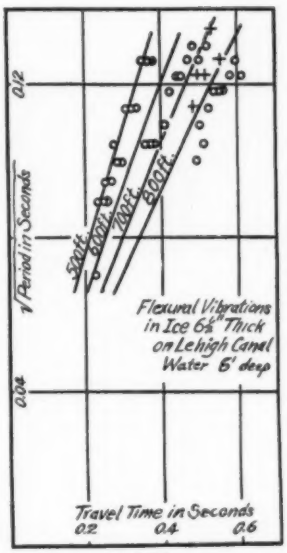

Fig. 3

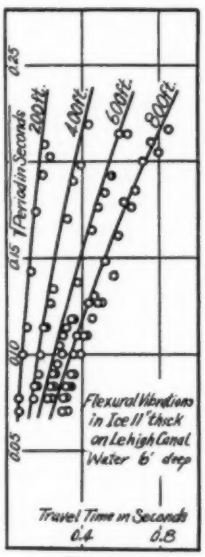

Fig. 4

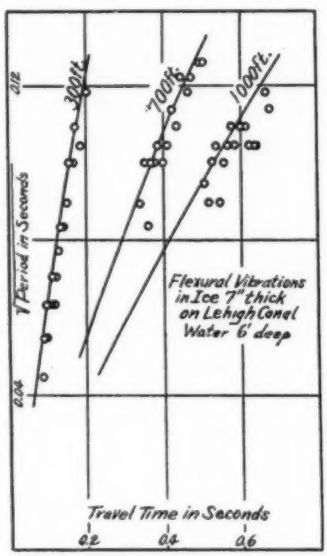

Fig. 5

Fig. 6

FIGS. 2 TO 6. Variation of group velocity of flexural vibrations in ice with frequency.

water. The value of the group velocity for the ice alone is also calculated from (5) and that from the general formula, (11) is compared with the data observed, as taken from (1). At higher frequencies the deviation amounts to almost 8 percent.

Three components of the motion in these flexural waves have been measured in several cases. This was accomplished by using three different orientations of the geophone; vertical, longitudinal and transverse. In the vertical orientation it measured vertical motion, in the longitudinal orientation it measured horizontal motion along the line of propagation of the waves, and in the transverse orientation it measured horizontal motion perpendicular to the direction of propagation. Since the sensitivity and damping ratio of geophone were not the same in the horizontal orientation as in the vertical only qualitative comparison of the different components of motion are possible. In the theoretical treatment of flexural waves the motion of the ice was assumed

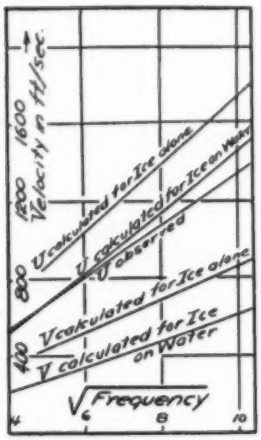

FIG. 7. Effect of presence of the water upon wave and group velocities of flexural vibrations in ice 4½ in. thick at Saylor's Lake.

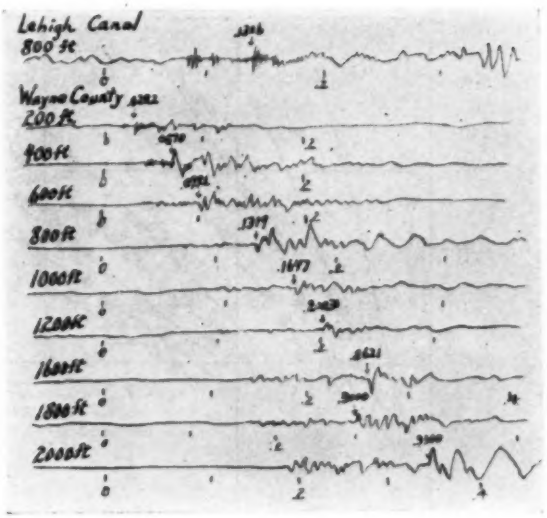

FIG. 8. Sample seismograms of transverse vibrations.

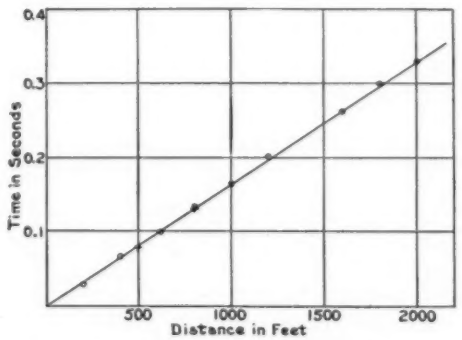

FIG. 9. Time distance curve for transverse vibrations in ice.

to be vertical. These waves were discovered, however, in the course of the investigation on longitudinal waves[1] in which the geophone was in the longitudinal orientation. Most of the data are for this orientation. Subsequent tests in which all three orientations were used showed the vertical component of motion to be greater than the horizontal ones, but still of the same order of magnitude. It appears that the longitudinal and vertical components are in phase for some records and 180° out of phase for others. This relation between the phases may be due to inaccurate levelling. The data available are inadequate to justify definite conclusions about these points.

TRANSVERSE VIBRATIONS

Transverse waves, in which the motion was horizontal and at right angles to the direction of propagation, were recorded in the ice on a frozen pond in Wayne County, Pennsylvania, and also on the Lehigh Canal. In these experiments the geophone was placed in the transverse orientation as described above. Tracings of the records are shown in Fig. 8. A plot of travel time against distance is shown in Fig. 9. By the method of least squares the velocity of transverse waves was determined from the data to be 6057 ± 15 ft./sec.

The velocity of transverse waves in a plate is given by the same formula as the velocity of torsional waves in a rod. The present velocity checks with that of 5840 ft./sec., previously obtained by the authors for torsional waves in a rod of ice,[1] to about 3 percent.

ACKNOWLEDGMENTS

We are indebted to Messrs. A. M. Thorne, Jr. and J. M. Lohse for assistance in taking the observations, to the Trojan Powder Company for the explosives and to the Geophysical Research Corporation for the seismic instruments.

An Investigation of an Alternating-Current Method of Determining Critical Potentials

ROGER W. HICKMAN, *Cruft Laboratory, Harvard University*

(Received January 22, 1934)

An investigation of an alternating-current bridge method of measuring critical potentials in a vapor has been made. The tube containing mercury vapor and of similar structure to that used in the experiments of Franck and Hertz was placed in one arm of an impedance bridge and so arranged that a small alternating voltage in series with a small direct retarding voltage existed between the accelerating grid and collecting plate. Measurements of the equivalent variational plate resistance and reactance were made as the steady accelerating voltage was varied. Plots of the variational resistance or reactance, or the bridge balancing resistance or capacitance as a function of the accelerating voltage, showed the typical irregularities found in the ordinary current-voltage plots to be enhanced. The positions of the irregularities were found to be independent of the frequency and dependent on the amplitude of the applied alternating voltage within the range investigated. Results indicated that the resolving power of the method varies inversely with the amplitude of applied alternating voltage. The effect of vapor pressure on the position and evolution of the irregularities was also studied.

I. NATURE OF THE PROBLEM

THE object of the present work was to investigate the applicability of the alternating-current technique developed for measuring the variational coefficients of high-vacuum triodes to the determination of critical potentials. Following the work of Franck and Hertz[1] such determinations have usually been made from the break points appearing in the curve obtained by plotting the current to a collector electrode as a function of the voltage accelerating the electrons through the vapor. E. G. Dymond[2] has made such determinations from direct measurements of the slope of the current voltage curve. He used a deflection method involving the low frequency mechanical commutation of his galvanometer synchronously with a constant increment of voltage dV in series with the steady grid accelerating voltage. In the present work a null method was used in which a small audiofrequency voltage was superimposed on the steady retarding voltage between the grid and collector electrode.

In ordinary triodes it is well known[3] that if one considers the plate current i_p to be a function only of the plate and grid voltages (e_p and e_g) that

$$s_p = u_p k_p, \tag{1}$$

where

$$s_p = \left(\frac{\partial i_p}{\partial e_g}\right)_{e_p}, \quad u_p = -\left(\frac{\partial e_p}{\partial e_g}\right)_{i_p}, \quad k_p = \left(\frac{\partial i_p}{\partial e_p}\right)_{e_g}.$$

These three quantities are defined as the variational coefficients of the triode and each of them represents the slope or negative slope of some characteristic curve of the device. S_p for example is the slope of the familiar plate current-grid voltage curve. The typical galvanometer deflection *versus* accelerating voltage curve as obtained by Franck and Hertz and other workers using the inelastic impact method of determining critical potentials is simply the plate current-grid voltage characteristic of the tube under the appropriate conditions. An alternating-current or dynamic measurement of s_p, i.e., the slope of the plate current-grid voltage curve, under the same conditions should lead to better defined break points or changes in slope of the static curve. Measurements of s_p in high vacuum triodes may be made using either the method recently developed by Tuttle[4] or one of the methods given by Chaffee.[5] The former utilizes highly specialized apparatus developed for commercial tube testing and is not immediately adaptable to the present

[1] J. Franck and G. Hertz, Ber. d. Dtsch. Phys. Ges. **16**, 457 (1914).
[2] E. G. Dymond, Proc. Roy. Soc. **A107**, 291 (1925).
[3] E. L. Chaffee, *Theory of Therm. Vac. Tubes*—p. 165.
[4] W. N. Tuttle, Proc. I. R. E. **21**, 844 (1933).
[5] E. L. Chaffee, reference 3, Chap. IX.

problem. Of the other methods there is no single circuit available which will measure both the positive and negative values of s_p encountered in a tube containing gas. As hysteresis effects may be present in such tubes a single continuous circuit throughout the range of accelerating voltage is necessary. Inability to meet this requirement led to abandonment of the idea of measuring s_p. From (1) it is apparent that measurements of either u_p or k_p will serve equally well except for the less direct interpretation. Measurements of u_p were found to offer circuital difficulties similar to those encountered with $s_p \cdot K_p$ remains positive throughout the range of accelerating voltage and circuit complications are minimized since an ordinary impedance bridge will suffice for the measurements.

II. Experimental Arrangement

The tube was constructed with four cylindrical electrodes, equipotential heater type cathode, two grids and a plate. Most of the parts were obtained from the Raytheon Production Corporation of Newton, Massachusetts. Details of the tube structure are given in Table I. The electrodes were all one inch in length and mounted coaxially on a standard 24 type tube stem with mica supports at top and bottom and enclosed in a glass envelope. The central portion of the cathode was coated for 0.5 inch by a layer of barium and strontium carbonates. The tube elements and glass envelope were thoroughly denuded of gas and mercury introduced by a double distillation process. The tube was sealed from the pumps and placed in a thermostated oil bath whose temperature could be held constant to within ±0.05°C.

Table I. *Details of tube structure. Dimensions in inches.*

	Cathode	Inner grid	Outer grid	Plate
Material	Nickel	Molybdenum	Nickel	Nickel
Inside diam.	0.085	0.16	0.86	1.0
Stock	0.0015	0.005	0.012	60×60 mesh
Turns per inch	. . .	29.5	32	. . .

Fig. 1 shows the connections. The d.c. circuit is essentially a duplication of the simplest circuit which has been used in the detection of critical potentials. This circuit of admittedly low resolving power was chosen purposely to show the advantages of the alternating-current method. With the inner grid held constant at a small positive potential with respect to the cathode the number of the tube elements was effectively reduced from four to three as it functioned as a virtual cathode. The main accelerating voltage was applied between the two grids, while a small fixed retarding voltage in series with the a.c. measuring voltage existed between the outer grid and plate. A small alternating voltage of the order of a few hundredths volt was applied through a shielded transformer to the terminals of the impedance bridge. Choke coils shunting the voltage source and amplifier provided low resistance paths for the d.c. plate current. Large by-pass condensers maintained the cathode and both grids at the same alternating potential.

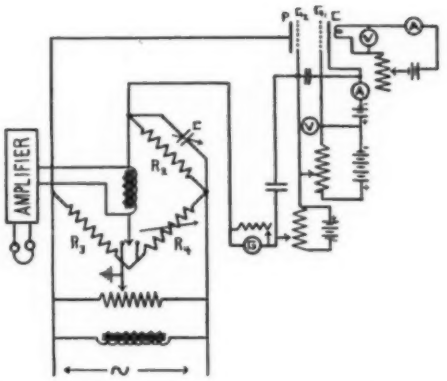

Fig. 1. Circuit diagram of the experimental arrangement.

Fig. 2 shows (a) the schematic a.c. circuit including the tube, (b) the complete equivalent circuit resulting from application of the equivalent plate and grid circuit theorems[6] and (c) the final simplified form. The simple bridge network results since the grid-filament capacitance is shorted; the plate-filament and grid-plate capacitances are in parallel as indicated by C_m; $u_p e_g$ is zero since e_g is zero and $u_g e_p$ is entirely dissipated in the variational grid resistance. At balance the equation $Z_1 Z_4 = Z_2 Z_3$ is valid, where Z_1 is the equivalent variational impedance between the elements P and F, Z_2 is the equiva-

[6] E. L. Chaffee, reference 3, Chap. VIII.

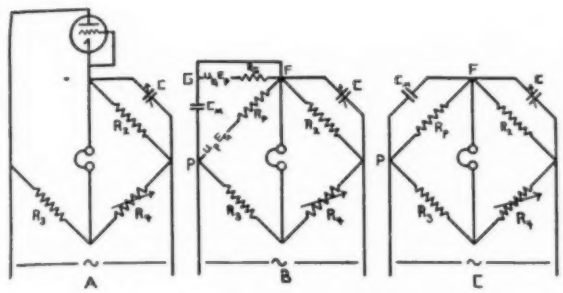

FIG. 2. Schematic alternating-current circuits. *A*, fundamental circuit including tube; *B*, circuit resulting when equivalent plate and grid circuit theorems are applied; *C*, final simplified circuit.

lent series impedance of R_2 and C in parallel, and Z_3 and Z_4 are pure resistances. The equivalent variational resistance and reactance between P and F will be designated by (r_p) and (x_p), respectively; similarly (R_2) and (X_2) for the arm containing R_2 and C. The balance condition given above yields the expressions,

$$(r_p)=\frac{(R_2)R_3}{R_4} \qquad (x_p)=\frac{R_3}{R_4}(x_2),$$

where

$$(R_2)=\frac{R_2}{1+(R_2C\omega)^2} \qquad (x_2)=\frac{-R_2^2C\omega}{1+(R_2C_2\omega)^2}.$$

III. Experimental Results

Fig. 3 shows typical results obtained by plotting both the bridge balancing resistance R_4 and the current to the plate as recorded simultaneously against the accelerating voltage measured from the space charge grid. Comparison of plots of (r_p), (x_p), R_4 and C against the accelerating voltage showed that the break points always occurred at the same value of voltage and could be determined as easily from one curve as another. All results are shown plotted in terms of R_4. The current curve I, in Fig. 3, shows the typical 4.9 volt separation of maxima corresponding to the voltage difference required to produce the first excited state of mercury independent of the initial velocity of emission and contact potentials existing in the apparatus. The resistance curve R, shows analogously two much sharper maxima and in addition auxiliary maxima and irregularities which are not evident in the current curve. A lateral displacement of

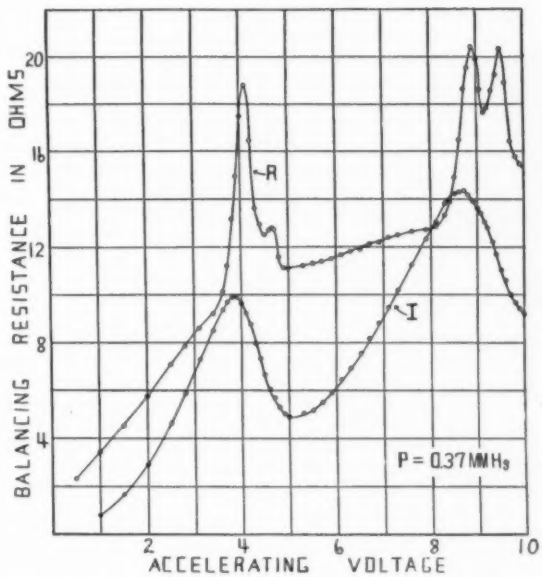

FIG. 3. Typical curves taken simultaneously showing direct-current galvanometer deflection and the alternating-current bridge balancing resistance plotted against the accelerating voltage. The same scale of ordinates applies to both curves.

the two curves is observed. Fig. 4 indicates how this displacement may arise. The quantity (k_p) or $1/(r_p)$ to which R_4 is approximately proportional can be computed from two static curves as shown. These two curves were taken for two different values of retarding voltage. For any value of the accelerating voltage e_g, (k_p) will be given by the difference of the ordinates of the two curves at the point in question divided by the difference of the two values of (E_g-E_p) for which the two curves were taken. This shows that the current and (k_p) curves would have their maxima at the same value of accelerating voltage only under the condition that the two current curves taken for the different values of retarding voltage be symmetrical in a small region near their peaks. If this were not true the quantity a of Fig. 4 could be larger at some other voltage than that of the peak of the current curves. It is also evident from this figure that a single plate current curve taken at the same time that dynamic measurements are made cannot be taken as a basis of interpretation of the latter. The space model of Fig. 5 emphasizes this point in an alternate manner. If one assumes that $I_p=f(E_p, E_g)$ then I_p for a given cathode

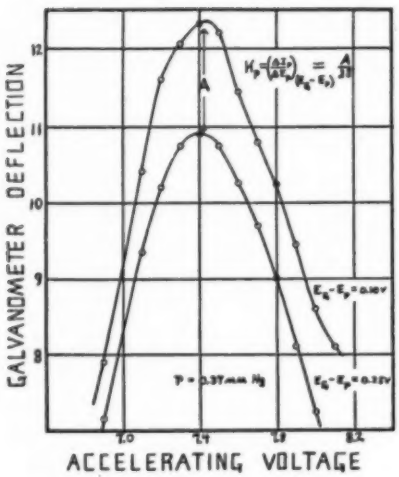

FIG. 4. Static curves from which the quantity which is measured dynamically may be derived.

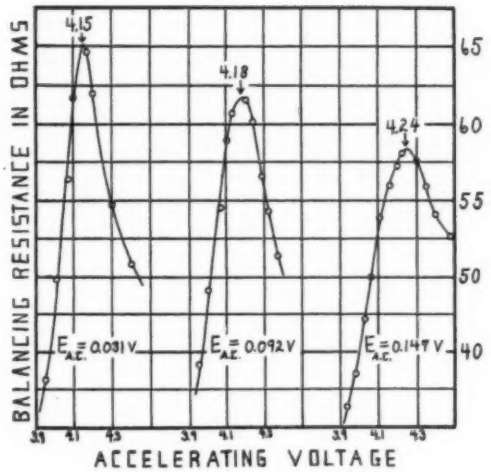

FIG. 6. Curves illustrating three effects of variation in amplitude of the applied alternating voltage; (1) lateral shift of the maximum, (2) broadening of maximum with increased amplitude, (3) change in magnitude of maximum.

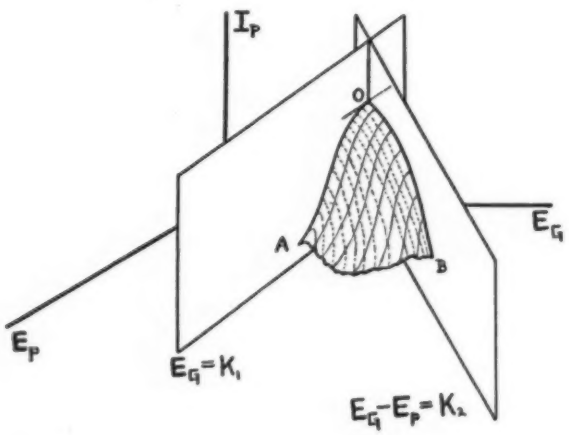

FIG. 5. Geometric interpretation employing a characteristic surface. The method measures the slope of the curve AO in the plane $E_g=k_1$ at its point of intersection O with the plane $E_g-E_p=k_2$.

temperature may be represented by a characteristic surface in space. Let the surface be cut by the planes $E_g=k_1$ and $E_g-E_p=k_2$. Then the alternating-current or dynamic method used measures the slope of the curve AO in the plane $E_g=k_1$ at its point of intersection O with the plane $(E_g-E_p)=k_2$. Observations of the slope were made as the plane $E_g=k_1$ was moved by small intervals through the characteristic surface and parallel to the I_pE_p plane. Again it is evident that no single current curve may be used as a basis for interpretation of the k_p curve.

Investigation was made of the effect of varying the amplitude of the alternating voltage applied to the bridge by making a series of measurements in the neighborhood of the first maximum of the resistance curve. Typical results are shown in Fig. 6. They show that an increase in amplitude of the measuring voltage causes the maximum to be shifted slightly, broadened and changed in magnitude. Careful tests showed that the separation of related maxima, e.g., the two main peaks in the resistance curve of Fig. 3, did not change with the amplitude of the measuring voltage. The broadening with amplitude implies clearly that the condition for the highest resolution of adjacent maxima is that as small an amplitude of measuring voltage be used as is consistent with the required bridge sensitivity. The change in magnitude of the maximum could not be predicted a priori as it can be shown experimentally that it depends on the shape of the curve whose slope is being sought. Fig. 7, (a) and (b), illustrates this. The plate-current grid-voltage characteristic of a typical high-vacuum triode is shown at (a). At (b) are shown two curves representing the dynamically determined slopes of the characteristic curve taken at the points 1 and 2 as a function of the alternating voltage applied to the circuit. The curves indicate clearly that the magnitude of the slope determined dynamically approaches a definite value

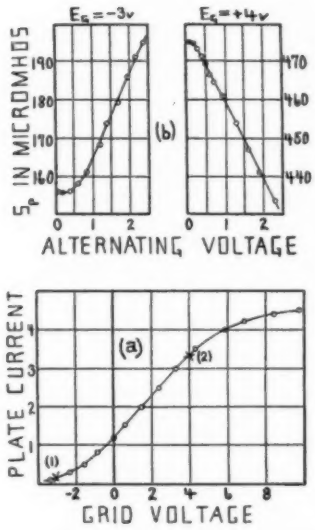

FIG. 7. Curves showing that an increase or a decrease in magnitude of slopes determined dynamically as a function of the applied a.c. voltage depends on the shape of the current-voltage characteristic at the point in question.

asymptotically as the amplitude of the alternating measuring voltage approaches zero. Whether it increases or decreases as one departs from small amplitudes depends on the shape of the current curve.

With a fixed amplitude of applied alternating voltage measurements were made using frequencies of 500, 750, 1000, 1500 and 2000 c.p.s. In all cases the position of the first main maximum of the resistance curve about which tests were made, occurred within ± 0.01 volt of the same value. Such a result would be expected as the time of flight of the carriers in the tube is very small compared with the period of the applied alternating voltage. The frequency range investigated was restricted to this narrow band as being that most applicable to the utilization of telephone receivers as the null indicator.

To test the method further measurements were made when the vapor pressure in the tube was varied. Effects of this variation of pressure are tied up inherently with any variable space charge effects introduced by different cathode temperatures as it was found impossible to make measurements satisfactorily over a wide pressure range using the same cathode heater voltage. As the pressure varied from 0.68 to 0.045 mm of Hg the cathode heater voltage was varied between 1.73 and 1.50 volts. Attempts to employ the same cathode heater voltage at the highest pressure as had been used at the lowest were vitiated by the smallness of the plate current while attempts to use the highest heater voltage at the lowest pressure resulted in conditions of instability. At no time during the course of measurements was there evidence of oscillations within the tube which might give rise to instability or spurious results. Such oscillations have been observed by the writer in other tubes containing mercury vapor but are believed to have played no part in the present work.

The results obtained at various pressures are shown in Fig. 8. The curve taken at the lowest pressure shows an irregularity of a different type than the others. The broad maximum which occurs at 2 volts disappears entirely as one goes to higher and higher pressures. If this maximum were due to a characteristic of the vapor in the tube it should be possible to observe it at approximately the same value of accelerating voltage for various heater voltages, when the pressure is held constant. Experiments showed however that it shifted and finally disappeared as the heater voltage was increased and as it had in no case the sharpness of the maxima which are characteristic of the vapor it was concluded that it was a function of the tube structure. Data taken on a tube of similar structure containing no mercury vapor confirmed this conclusion.

In Fig. 8 the curve for $p = 0.68$ mm of Hg shows two main maxima separated by a voltage of 4.8 volts, corresponding approximately to the first excitation potential of mercury. These two maxima as well as those 0.6 volt to their right may be observed on each of the curves. The evolution of these maxima is of interest. Referring to them as 1, 2, 3 and 4 as indicated, it is apparent that 2 and 4 rapidly increase in prominence as the pressure is decreased until 1 is a mere kink on the side of 2, 3 is still evident and 4 as a separate maximum has entirely disappeared.

If the scheme used by other workers in this field for correcting the voltage scale is adopted a possible explanation of the maxima and irregularities of this family of curves may be given. Customarily the voltage separation of the first two main current maxima, corresponding to the lowest excitation potential, is assigned to the

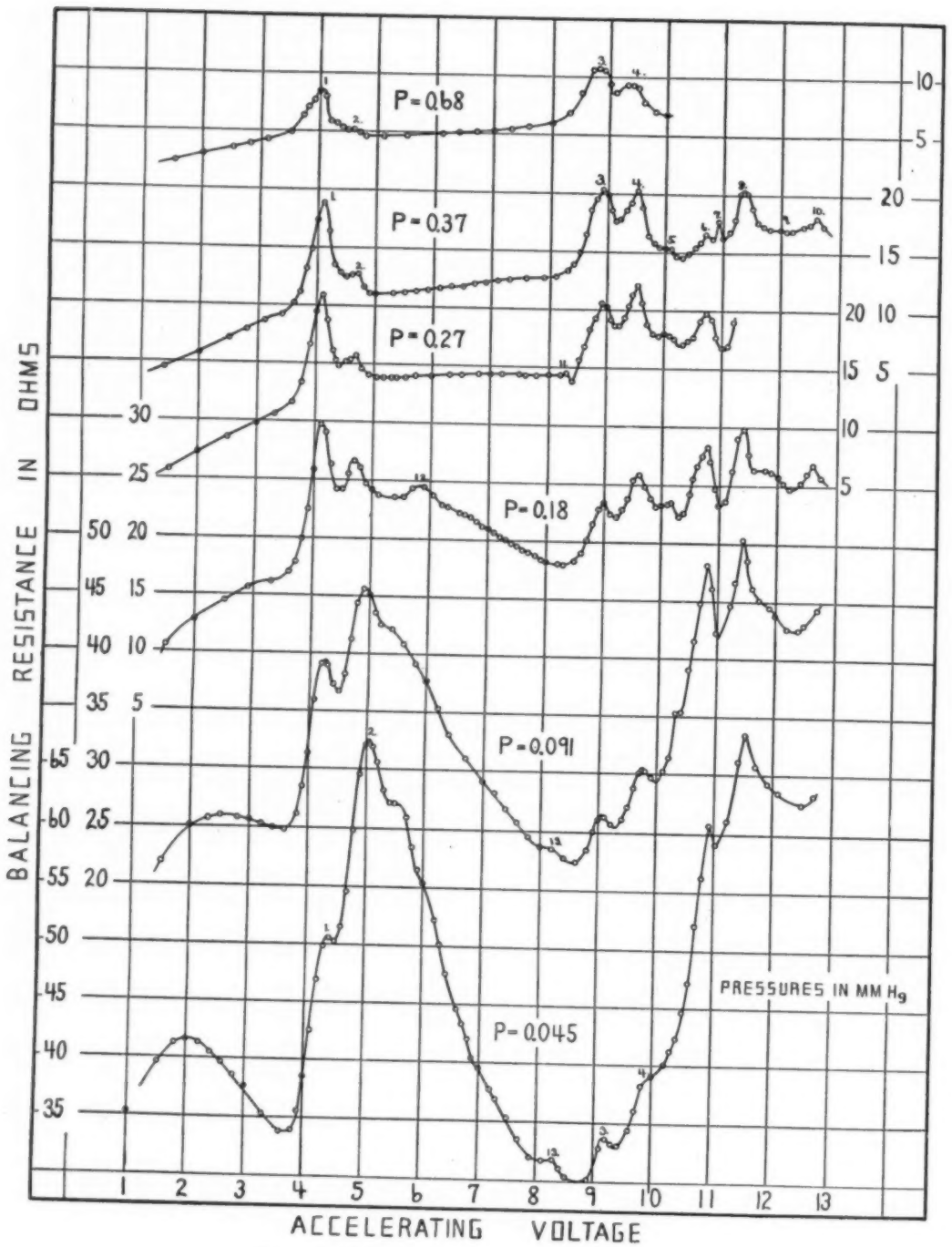

FIG. 8. Results obtained at various pressures.

first maximum and the voltage of other irregularities determined from this. Assigning a value of 4.9 volts to 1 we find that 2 occurs at approximately 5.5 volts. This may correspond either to direct excitation of the 5.43 volt energy level, or to ionization of atoms which are in the 4.9 volt state as has been suggested by Compton and Mohler,[7] or both processes might contribute to the observed effect. The prominence of this maximum occurring always very definitely at 0.6 volt beyond the 4.9 volt peak is not easily explained without regarding ionization of atoms in the 4.9 volt state as a contributory factor. The emission characteristics of the tube indicated that measurements were made in the presence of some space charge and its neutralization by the formation of a few positive ions would explain the enhanced irregularity observed. The maxima 3 and 4 may be similarly explained except that they are caused by electrons which have already made one inelastic collision.

All of the main irregularities of the curves of Fig. 8 may be identified with some critical potential or combination of one or more. As an example take the curve for $P=0.37$ mm of Hg and adopt the scheme of Einsporn[8] for presenting the possible explanation. The required excitation energies in volts will be abbreviated as follows; $a=4.7$, excitation of 4.66 v level, $b=4.9$, excitation of 4.88 v level, $c=6.7$ excitation of 6.67 v level, $d=5.4$ or 5.5, corresponding either to excitation of the 5.43 v level or ionization of the 4.9 v state, $e=5.7$, ionization of the 4.7 v metastable state, $f=6.0$, a break point reported by Franck and Einsporn to which apparently no atomic energy level corresponds. The break points or maxima and their explanation in terms of the above are given in Table II.

TABLE II. *Refers to Fig. 8. $P=0.37$ mm of Hg. Interpretation of maxima in terms of the following excitation energies in volts; $a=4.7$, $b=4.9$, $c=6.7$, $d=5.4$ or 5.5, $e=5.7$, $f=6.0$.*

No.	Obs. break point in volts	Corrected voltage	Explanation voltage calc.	Discrepancy ΔV
1	4.1	4.9	$b=4.9$	0
2	4.7	5.5	$d=5.4$ or 5.5	0 or 0.1
3	8.9	9.7	$2b=9.8$	0.1
4	9.5	10.3	$b+d=10.3$ or 10.4	0 or 0.1
5	10.1	10.9	$2d=10.8$ or 11.0	0.1
6	10.7	11.5	$a+c=11.4$	0.1
7	10.9	11.7	$b+c=11.6$	0.1
8	11.35	12.15	$c+d=12.1$ or 12.2	0.05
9	12.0	12.8	$c+f=12.7$	0.1
10	12.6	13.4	$2c=13.4$	0

The curves obtained at lower pressures show in addition direct excitation of the 6.67 and 8.8 volt energy levels. These results agree with previous work in that the higher levels are determined at the lower pressures where the lengthened mean free path enables the electrons to acquire more energy between impacts for a given potential gradient.

Because of the high resolving power of the method when applied to the poorest of d.c. circuits it is proposed to continue the work by applying the a.c. technique to one of the d.c. circuits of high sensitivity and resolving power.

This work was carried out under the direction of Professor E. L. Chaffee to whom it is a pleasure to acknowledge the many suggestions and encouragement offered during the course of the work. The writer also desires to acknowledge the interest and kindly criticism of Professor O. Oldenberg.

[7] Compton and Mohler, Bulletin of the Nat. Research Council **48**, 10 (1924).
[8] E. Einsporn, Zeits. f. Physik **5**, 208 (1921).

Notice to Contributors

Manuscripts

Send manuscripts to John T. Tate, University of Minnesota, Minneapolis, Minnesota.

Papers must be in English, typewritten double spaced with wide margins.

Abstracts

An abstract must accompany each article. It should be adequate as an *index* and as a *summary*. As an index it should give all subjects, major and minor, concerning which new information is presented. As a summary it should give the conclusions of the article and all numerical results of general interest.

References

References should appear as foot notes, numbered consecutively, and arranged thus:

A. B. Smith, Phys. Rev. **41**, 852 (1932).

Captions and Legends

Legends for figures must accompany manuscript. Each table should have a caption. These in all cases should be complete in themselves so as to make the data intelligible to the reader without reference to the text.

Mathematical Expressions

Make all expressions clear to the typesetter. Identify in the margin of the manuscript Greek letters and unusual symbols.

Use fractional exponents instead of root signs.

Avoid complicated exponents and subscripts. Should it be necessary to repeat a complicated expression a number of times it should be represented by some convenient symbol.

The solidus (/) should be used wherever possible for fractions.

Illustrations

Plan figures for approximately one-half reduction. Wherever possible arrange figures so that after reduction they will not be wider than three inches. Lettering must be large enough to be readable after reduction.

Line drawings must be made with India ink on white paper or tracing cloth. Coordinate paper is not desirable, but if used must be blue-lined and all coordinates to be reproduced drawn with India ink.

Drawings which cannot be used will be returned to the author or redrawn at his expense.

Photographs should show clear black and white contrasts.

Avoid round and oval photographs.

Publication Charge

A portion of the cost of publishing the results of research must be regarded as an integral part of the cost of the research. In keeping with the policy which is effective for the Institute's publications a bill for $3.00 per page will be sent to the authors of papers appearing in this journal. It is intended that the authors shall present these bills for payment to the institutions which have supported their researches. If the institution is unable to make payment the bills are to be returned marked "No Funds Available."

Reprints

As a partial return for the publication charge one hundred reprints without covers will be furnished free. Additional reprints may be obtained at a regular schedule of prices.

Alterations

Take great care that each manuscript is typographically accurate. A limited number of alterations in proof are unavoidable, but the cost of making extensive alterations after the article has been set in type will be charged to the author.

Proof and all correspondence concerning papers in the process of publication should be addressed to the Editorial Secretary, American Institute of Physics, 11 East 38th Street, New York, N. Y.

THE AMERICAN PHYSICAL SOCIETY

ARTHUR H. COMPTON, *President*
University of Chicago
Chicago, Illinois

R. W. WOOD, *Vice-President*
The Johns Hopkins University
Baltimore, Maryland

W. L. SEVERINGHAUS, *Secretary*
Columbia University
New York, New York

G. B. PEGRAM, *Treasurer*
Columbia University
New York, New York

JOHN T. TATE, *Editor*
University of Minnesota
Minneapolis, Minnesota

L. B. LOEB, *Local Secretary for the Pacific Coast*
University of California
Berkeley, California

THE object of the American Physical Society is the advancement and diffusion of the knowledge of physics. It sponsors *The Physical Review*, *Physics* and the *Reviews of Modern Physics*. Upon the recommendation of two or more members, any person engaged in work in the field of physics or actively interested in physics may become a member; receive one of the journals; receive also *Science Abstracts* A, *The Review of Scientific Instruments with Physics News and Views*, and the Bulletin of all meetings; and attend and participate in the seven annual meetings.

Annual dues: $10. Fellows, $14.

For further information address the Secretary as above.

THE SOCIETY OF RHEOLOGY

S. E. SHEPPARD, *President*
Eastman Kodak Company
Rochester, New York

EUGENE C. BINGHAM, *Editor*
Lafayette College
Easton, Pennsylvania

A. STUART HUNTER, *Secretary & Treasurer*
Du Pont Rayon Company
Buffalo, New York

THE Society of Rheology was formed in 1929 to advance the science of the deformation and flow of matter. It cooperates with the American Physical Society in editing *Physics* of which four issues per year are devoted to *Rheology*. All persons interested are invited to become members and participate in the proceedings at the annual December meetings. Members receive without other charge than their dues all issues of *Physics*, *The Review of Scientific Instruments with Physics News and Views* and the notices of the Society.

Annual dues: $6.

For further information address the Secretary as above.